Sliding Mode Controls of Double-Pendulum Crane Systems

Article *in* Journal of Mechanical Science and Technology · June 2013

DOI: 10.1007/s12206-013-0437-8

2 authors:

Le Anh Tuan
Vietnam Maritime University
27 PUBLICATIONS **794** CITATIONS
SEE PROFILE

Soon-Geul Lee
Kyung Hee University
166 PUBLICATIONS **1,627** CITATIONS
SEE PROFILE

Springer

KSME

Journal of Mechanical Science and Technology 27 (6) (2013) 1863~1873
www.springerlink.com/content/1738-494x
DOI 10.1007/s12206-013-0437-8

Sliding mode controls of double-pendulum crane systems †

Le Anh Tuan[1] and Soon-Geul Lee[2,*]

[1]*Reseach and Development Center, Duy Tan University, Da Nang city, Vietnam*
[2]*Department of Mechanical Engineering, Kyung Hee University, Yongin-si, Gyeonggi-do, 446-701, Korea*

(Manuscript Received July 7, 2012; Revised January 23, 2013; Accepted February 13, 2013)

Abstract

This study focuses on the design of robust nonlinear controllers based on both conventional and hierarchical sliding mode techniques for double-pendulum overhead crane systems. In the first approach, a first-order sliding surface is provided and a proper control scheme is generated to stabilize the surface. In the second approach, two levels of sliding surfaces are proposed and the control scheme is designed based on the stability of the second-level surface. We also prove the stability of the first-level sliding surface. To verify the quality of the proposed controllers, simulation for a particular type of overhead crane systems is implemented. Simulation results show that all state trajectories asymptotically converged to desired values.

Keywords: Lyapunov function; Overhead crane; Sliding mode control; Switching surface

1. Introduction

Overhead cranes are frequently used in a number of industrial fields to transfer cargo over a short distance. Productivity of cranes and their operating safety depend greatly on the skills of the operator. Therefore, control of overhead cranes composed of both anti-swing and tracking controls is an important engineering problem that has attracted the attention of numerous researchers. Linear control problems [1-3] of crane systems have been sufficiently treated. Numerous studies concerning nonlinear control [4-6] of overhead cranes using various techniques such as feedback linearization [7-10] and Lyapunov-based methods [11-15] have been reported. However, these nonlinear control problems still have imperfect solutions. In this study, we design robust nonlinear controllers of overhead cranes based on variable structure control approaches, also called sliding mode control (SMC) techniques. General theory of SMC for a class of under-actuated systems was introduced by Lee [16], developed by Ashrafiuon [17], and completed by Sankaranarayanan [18]. Subsequently, a series of control crane papers using SMC was published. Karkoub [19] introduced a variable structure controller in conjunction with a state feedback control scheme and a μ-synthesis control scheme. Bartolini [20] constructed two SMC schemes, a proportional-integral-based controller and a linear observer-based, time-varying feedback scheme. Ngo [21] discussed an SMC controller for container crane anti-sway. Bartolini [22] proposed a second-order sliding modes controller for two-dimensional overhead crane with a constant cable length. Lee [23] calculated a first-order SMC law to drive cargo swing and trolley motion concurrently. This scheme was derived from sliding surface stability analysis. Sliding surface was defined by linearly combining all state errors. Almutrairi [24] enhanced the study of Lee [23] and designed an SMC controller for a three-dimensional crane system, in which a lifting cargo, a traveling trolley, and a moving bridge are concurrently included. A modified version of SMC technique, called hierarchical sliding mode control (HSMC) [25-28], has likewise been applied. Wang [25] and Qian [26] developed HSMC technique for a class of single-input-multiple-output (SIMO) systems and applied this method to an overhead system and a pendulum as illustrated examples.

The aforementioned studies dealt with SMC control problems for overhead cranes in which hook mass is not included in the dynamic model. In this research, we concentrate on robust nonlinear control of an overhead crane system modeled as a moving double-pendulum by considering hook mass. Both conventional sliding mode control (CSMC) and its modified version, HSMC [25, 26], are used. SMC technique and its modified version have been applied widely in a number of realistic systems. These techniques are extremely useful for under-actuated systems with uncertainties, in which the num-

*Corresponding author. Tel.: +82 31 201 2506, Fax.: +82 31 202 1204
E-mail address: sglee@khu.ac.kr
† Recommended by Associate Editor Yang Shi

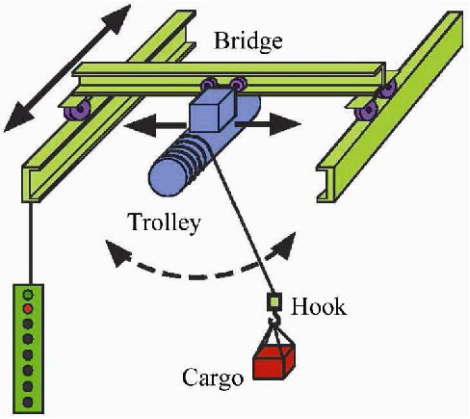

(a) Overhead crane system [29]

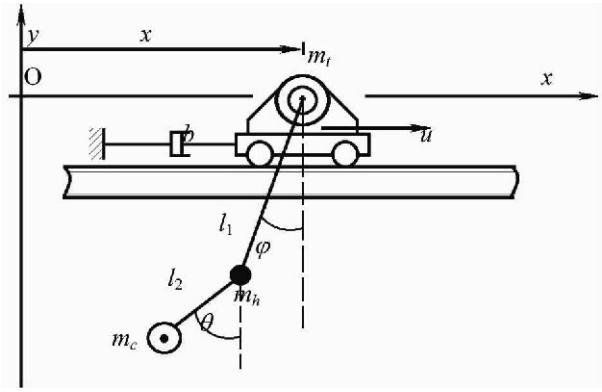

(b) Physical model

Fig. 1. Double-pendulum overhead crane system.

ber of outputs is greater than that of inputs. Generally, SMC design consists of two basic steps: defining proper manifold(s) and constituting robust control scheme involving switched actions. To stabilize the system, control inputs must pull system states to switching manifold and slide them to desired positions on these manifolds. The pulling phase is normally sensitive and the sliding phase is insensitive with variations resulting from uncertainties and disturbances. Thus, the period of pulling (reaching) phase should be reduced and should be as short as possible. In CSMC, we determine a common first-order sliding surface for state variables and generate control input to attract all system states to this surface. In HSMC, sliding surfaces are individually defined for three subsystems because total system dynamics is divided into three parts corresponding to the three pairs of state variables (displacement and its derivative). Next, we define a first-level sliding surface involving three components, in which each component corresponds to each pair of state variables. A second-level sliding surface is provided by linearly combining the three components of the first level. The control scheme is then designed based on the stability of the second-level manifold. Finally, we analyze stability of the first-level manifold. In this control problem for SIMO systems, the single control input acting as the trolley driving force must perform three duties: precisely tracking the trolley from its initial position to the desired point while simultaneously keeping swing angles of cargo and hook minimal during the transfer process, and totally suppressing them at payload destination.

This paper is organized as follows. Section 2 introduces the mathematical model of an overhead crane system composed of three fully nonlinear, differential, highly coupled equations. Traditional SMC will be applied to design a robust controller in section 3. In section 4, we construct the other robust controller using multi-level sliding mode technique. To obtain responses from the crane system driven by the proposed controllers, simulation is carried out and its results are presented in section 5. Finally, conclusions are drawn in section 6.

2. System modeling

The overhead crane handling the cargo depicted in Fig. 1(a) [29] is considered. The cargo is normally suspended on the cable by a hook. If the hook mass m_h is included, then the physical model of the crane system can be viewed as a moving double-pendulum described in Fig. 1(b). The system has three concentrated masses composed of trolley mass m_t, cargo mass m_c, and m_h. Three generalized coordinates, which correspond to the three degrees of freedom, are chosen: θ denotes swing angle of hook, φ is swing angle of the cargo, and x indicates trolley displacement.

In this study, we analyze the control problem of the crane system in the case where only the trolley moving mechanism is operated and driven by force u. Without the hoisting mechanism, lengths of cables l_1 and l_2 are considered as constants. An assumption is made that motion trajectories of all components of the crane system are considered only on the Oxy plane. Based on virtual work principle and Lagrange's equation, the dynamics of a SIMO crane system can be described as follows:

$$\begin{pmatrix} (m_t+m_h+m_c)\ddot{x}-(m_h+m_c)l_1\cos\varphi\ddot{\varphi} \\ -m_c l_2\cos\theta\ddot{\theta}+b\dot{x}+(m_h+m_c)l_1\sin\varphi\dot{\varphi}^2 \\ +m_c l_2\sin\theta\dot{\theta}^2 \end{pmatrix}=u \tag{1}$$

$$\begin{pmatrix} -(m_h+m_c)l_1\cos\varphi\ddot{x}+(m_h+m_c)l_1^2\ddot{\varphi} \\ +m_c l_1 l_2\cos(\varphi-\theta)\ddot{\theta}+m_c l_1 l_2\sin(\varphi-\theta)\dot{\theta}^2 \\ +(m_h+m_c)gl_1\sin\varphi \end{pmatrix}=0 \tag{2}$$

$$\begin{pmatrix} -m_c l_2\cos\theta\ddot{x}+m_c l_1 l_2\cos(\varphi-\theta)\ddot{\varphi}+m_c l_2^2\ddot{\theta} \\ -m_c l_1 l_2\sin(\varphi-\theta)\dot{\varphi}^2+m_c g l_2\sin\theta \end{pmatrix}=0 \tag{3}$$

which can be rewritten in matrix form as

$$\mathbf{M}(\mathbf{q})\ddot{\mathbf{q}}+\mathbf{C}(\mathbf{q},\dot{\mathbf{q}})\dot{\mathbf{q}}+\mathbf{G}(\mathbf{q})=\mathbf{U} \tag{4}$$

with $\mathbf{q}=\begin{bmatrix}x & \varphi & \theta\end{bmatrix}^T$, being a coordinate vector, and $\mathbf{U}=\begin{bmatrix}u & 0 & 0\end{bmatrix}^T$, being a control force vector of the system.

$\mathbf{M}(\mathbf{q}) = \mathbf{M}^T(\mathbf{q})$ denotes a symmetric mass matrix given by

$$\mathbf{M}(\mathbf{q}) = \begin{bmatrix} m_t + m_h + m_c & -(m_h + m_c) l_1 \cos\varphi & -m_c l_2 \cos\theta \\ -(m_h + m_c) l_1 \cos\varphi & (m_h + m_c) l_1^2 & m_c l_1 l_2 \cos(\varphi - \theta) \\ -m_c l_2 \cos\theta & m_c l_1 l_2 \cos(\varphi - \theta) & m_c l_2^2 \end{bmatrix}.$$

$\mathbf{C}(\mathbf{q}, \dot{\mathbf{q}})$ is a damping and centrifugal matrix determined by

$$\mathbf{C}(\mathbf{q}, \dot{\mathbf{q}}) = \begin{bmatrix} b & (m_h + m_c) l_1 \sin\varphi\dot{\varphi} & m_c l_2 \sin\theta\dot{\theta} \\ 0 & 0 & +m_c l_1 l_2 \sin(\varphi - \theta)\dot{\theta} \\ 0 & -m_c l_1 l_2 \sin(\varphi - \theta)\dot{\varphi} & 0 \end{bmatrix}.$$

$\mathbf{G}(\mathbf{q})$ is a gravity matrix with the form

$$\mathbf{G}(\mathbf{q}) = \begin{bmatrix} 0 \\ (m_h + m_c) g l_1 \sin\varphi \\ m_c g l_2 \sin\theta \end{bmatrix}.$$

Physically, the cargo and hook can return to stable equilibrium point $\mathbf{q}_0 = [x_d \quad 0 \quad 0]^T$ through gravity without control. However, the swings of the cargo and hook can be decreased faster or slower, depending on the ability of the operator. The main objective of this study is to construct a proper control law u so that cargo and hook swings are kept small during the transfer process and completely vanished as fast as possible. Concurrently, trolley is driven to stop precisely at its destination. Based on system dynamics Eq. (4), controller design will be presented in the next sections.

3. CSMC design

3.1 Control scheme

The main objective of this section is to design a CSMC-based controller that can force the trolley to move to desired position x_d, and cargo and hook swing angles to completely vanish at payload destination. This design means that state variables $\mathbf{q} = [x \quad \varphi \quad \theta]^T$ will reach their desired values $\mathbf{q}_d = [x_d \quad 0 \quad 0]^T$ after minimum time. By assuming that all system states and their first-order derivatives are measurable, a sliding surface is defined as

$$s = \dot{e} + \lambda e + \alpha\varphi + \beta\theta \tag{5}$$

with $e = (x - x_d)$ being the tracking error of trolley motion; and λ, α, and β being design parameters.

CSMC design is based on making and retaining the value of switching surface s to be equally zero by means of discontinuous control acting on the first-order derivative of s, and switching between high amplitude opposite values with high frequency [30]. By taking $\dot{s} = 0$, we obtain

$$\dot{s} = \ddot{x} + \lambda\dot{x} + \alpha\dot{\varphi} + \beta\dot{\theta} = 0. \tag{6}$$

By inserting Eq. (1) into Eq. (6), we obtain the equivalent control input

$$u_{eq} = \begin{pmatrix} -(m_h + m_c) l_1 \cos\varphi\ddot{\varphi} - m_c l_2 \cos\theta\ddot{\theta} + b\dot{x} \\ +(m_h + m_c) l_1 \sin\varphi\dot{\varphi}^2 + m_c l_2 \sin\theta\dot{\theta}^2 \\ -(m_t + m_h + m_c)(\lambda\dot{x} + \alpha\dot{\varphi} + \beta\dot{\theta}) \end{pmatrix}. \tag{7}$$

The equivalent input Eq. (7) causes all state trajectories to reach the sliding surface. However, to keep these system states on the sliding manifold, switching action should be added to expression Eq. (7) as

$$\begin{aligned} u = & -(m_h + m_c) l_1 \cos\varphi\ddot{\varphi} - m_c l_2 \cos\theta\ddot{\theta} + b\dot{x} \\ & + (m_h + m_c) l_1 \sin\varphi\dot{\varphi}^2 + m_c l_2 \sin\theta\dot{\theta}^2 \\ & - (m_t + m_h + m_c)(\lambda\dot{x} + \alpha\dot{\varphi} + \beta\dot{\theta}) - K\,\mathrm{sgn}(s) \end{aligned} \tag{8}$$

where K is a high amplitude of switching gain, and sgn(s) denotes a sign function with the form

$$\mathrm{sgn}(s) = \begin{cases} 1 & \text{if } s > 0 \\ 0 & \text{if } s = 0 \\ -1 & \text{if } s < 0 \end{cases}. \tag{9}$$

A switching action normally causes chattering of state trajectories around the switching surface. To reduce chattering, sgn(s) function should be replaced by a saturation function as follows:

$$\mathrm{sat}(s) = \begin{cases} 1 \text{ if } s/\varepsilon > 1 \\ s/\varepsilon \text{ if } -1 < s/\varepsilon < 1 \\ 1 \text{ if } s/\varepsilon < -1 \end{cases} \tag{10}$$

where ε is a constant indicating the thickness of the boundary layer.

3.2 Stability analysis

Stability of system dynamics Eq. (4) driven by SMC force Eq. (8) is analyzed. Asymptotical stability of the sliding surface is proven, and stability of tracking problem $\mathbf{q} \equiv \mathbf{q}_d$ is investigated. Lyapunov lower bounded function $V = 0.5s^2$ is considered, the derivative of which is determined as

$$\dot{V} = s\dot{s} = s(\ddot{x} + \lambda\dot{x} + \alpha\dot{\varphi} + \beta\dot{\theta}). \tag{11}$$

Substituting Eqs. (1) and (8) into Eq. (11) results in

$$\dot{V} = s\dot{s} = -s\frac{K}{(m_t + m_h + m_c)}\mathrm{sign}(s) \tag{12}$$

which implies that

$$\dot{V} = -\frac{K}{\left(m_t + m_h + m_c\right)}|s| . \tag{13}$$

The fact that $\dot{V} \le 0$ for every $K > 0$ is obvious. Alternatively, the derivative of $\dot{V}$ is

$$\ddot{V} = -\frac{K}{\left(m_t + m_h + m_c\right)}|\dot{s}| = -\frac{K^2}{\left(m_t + m_h + m_c\right)^2} . \tag{14}$$

Because $\ddot{V}$ is bounded, function $\dot{V}$ is uniformly continuous in time. Application of Barbalat's lemma indicates that $\lim_{t\to\infty}\dot{V} = 0$ yields $\lim_{t\to\infty} s = 0$. Thus, sliding surface s is asymptotically stable for every positive switching gain K. This finding means that all state trajectories are attracted to the aforementioned surface.

We can easily see from Eq. (5) that $\lim_{t\to\infty} s = 0$ is not a sufficient basis for concluding the convergence of system outputs $\mathbf{q} = \begin{bmatrix} x & \varphi & \theta \end{bmatrix}^T$. The idea that system responses $\mathbf{q}$ approach desired values $\mathbf{q}_d$ if controller gains are properly selected is proven. CSMC Eq. (8) is determined to force $\dot{s} = 0$. Condition Eq. (6) is rewritten as

$$\ddot{x} = -\lambda\dot{x} - \alpha\dot{\varphi} - \beta\dot{\theta} . \tag{15}$$

Inserting Eq. (15) into swing dynamics Eqs. (2) and (3) yields

$$\begin{pmatrix} \left(m_h + m_c\right)\cos\varphi\left(\lambda\dot{x} + \alpha\dot{\varphi} + \beta\dot{\theta}\right) + \left(m_h + m_c\right)l_1\ddot{\varphi} \\ + m_c l_2\cos\left(\varphi - \theta\right)\ddot{\theta} + m_c l_2\sin\left(\varphi - \theta\right)\dot{\theta}^2 \\ + \left(m_h + m_c\right)g\sin\varphi \end{pmatrix} = 0 \tag{16}$$

$$\begin{pmatrix} \cos\theta\left(\lambda\dot{x} + \alpha\dot{\varphi} + \beta\dot{\theta}\right) + l_1\cos\left(\varphi - \theta\right)\ddot{\varphi} \\ + l_2\ddot{\theta} - l_1\sin\left(\varphi - \theta\right)\dot{\varphi}^2 + g\sin\theta \end{pmatrix} = 0 . \tag{17}$$

By setting state variables

$$\begin{aligned} \mathbf{z} &= \begin{bmatrix} z_1 & z_2 & z_3 & z_4 & z_5 & z_6 \end{bmatrix}^T \\ &= \begin{bmatrix} e & \dot{e} & \varphi & \dot{\varphi} & \theta & \dot{\theta} \end{bmatrix}^T , \end{aligned}$$

the closed-loop system composed of Eqs. (15)-(17) become a nonlinear state-space system as follows

$$\dot{z}_1 = z_2 , \tag{18}$$

$$\dot{z}_2 = -\lambda z_2 - \alpha z_4 - \beta z_6 \tag{19}$$

$$\dot{z}_3 = z_4 , \tag{20}$$

$$\dot{z}_4 = \begin{pmatrix} -\frac{1}{l_1}\cos z_3\left(\lambda z_2 + \alpha z_4 + \beta z_6\right) \\ -\frac{m_c l_2}{\left(m_h + m_c\right)l_1}\cos\left(z_3 - z_5\right)\dot{z}_6 \\ -\frac{m_c l_2}{\left(m_h + m_c\right)l_1}\sin\left(z_3 - z_5\right)z_6^2 \\ -\frac{g}{l_1}\sin z_3 \end{pmatrix} = m\left(\mathbf{z}\right) \tag{21}$$

$$\dot{z}_5 = z_6 , \tag{22}$$

$$\dot{z}_6 = \begin{pmatrix} \frac{l_1}{l_2}\sin\left(z_3 - z_5\right)z_4^2 - \frac{g}{l_2}\sin z_5 \\ -\frac{1}{l_2}\cos z_5\left(\lambda z_2 + \alpha z_4 + \beta z_6\right) \\ -\frac{l_1}{l_2}\cos\left(z_3 - z_5\right)\dot{z}_4 \end{pmatrix} = n\left(\mathbf{z}\right) . \tag{23}$$

By linearizing the previously shown state-space system around equilibrium point $\mathbf{z}_0 = \mathbf{0}$, a linear system can be obtained:

$$\dot{\mathbf{z}} = \mathbf{A}\mathbf{z} \tag{24}$$

with **A** being a Jacobian matrix defined by

$$\begin{aligned} \mathbf{A} &= \begin{bmatrix} 0 & 1 & 0 & 0 & 0 & 0 \\ 0 & -\lambda & 0 & -\alpha & 0 & -\beta \\ 0 & 0 & 0 & 1 & 0 & 0 \\ \frac{\partial m(\mathbf{z})}{\partial z_1} & \frac{\partial m(\mathbf{z})}{\partial z_2} & \frac{\partial m(\mathbf{z})}{\partial z_3} & \frac{\partial m(\mathbf{z})}{\partial z_4} & \frac{\partial m(\mathbf{z})}{\partial z_5} & \frac{\partial m(\mathbf{z})}{\partial z_6} \\ 0 & 0 & 0 & 0 & 0 & 1 \\ \frac{\partial n(\mathbf{z})}{\partial z_1} & \frac{\partial n(\mathbf{z})}{\partial z_2} & \frac{\partial n(\mathbf{z})}{\partial z_3} & \frac{\partial n(\mathbf{z})}{\partial z_4} & \frac{\partial n(\mathbf{z})}{\partial z_5} & \frac{\partial n(\mathbf{z})}{\partial z_6} \end{bmatrix}_{\mathbf{z}=\mathbf{0}} \\ &= \begin{bmatrix} 0 & 1 & 0 & 0 & 0 & 0 \\ 0 & -\lambda & 0 & -\alpha & 0 & -\beta \\ 0 & 0 & 0 & 1 & 0 & 0 \\ 0 & -\frac{\lambda}{l_1} & -\frac{g}{l_1} & -\frac{\alpha}{l_1} & 0 & -\frac{\beta}{l_1} \\ 0 & 0 & 0 & 0 & 0 & 1 \\ 0 & -\frac{\lambda}{l_2} & 0 & -\frac{\alpha}{l_2} & -\frac{g}{l_2} & -\frac{\beta}{l_2} \end{bmatrix} . \end{aligned} \tag{25}$$

According to Lyapunov's linearization theorem [31], if the linearized system Eq. (24) is strictly stable, then the nonlinear system Eqs. (18)-(23) is asymptotically stable around the equilibrium point. For this case, **A** must be a Hurwitz matrix to satisfy stability of the system Eq. (24). This phenomenon leads to

$$\lambda > 0, \alpha > 0 \quad \text{and} \quad \beta < 0 \tag{26}$$

after several calculations based on Routh-Hurwitz criterion.

Thus, crane systems Eqs. (1)-(3) driven by CSMC input Eq. (8) are stable if the conditions Eq. (26) for controller gains are held.

4. HSMC design

To control the crane system based on HSMC technique [25-28], system dynamics is converted from one form to another. Dynamic behaviors of the crane system are characterized by highly coupled second-order differential nonlinear Eqs. (1)-(3),

in which only actuated Eq. (1) has an explicit relationship between state variables and control input u. By substituting Eq. (1) into Eq. (2) and (3), and then rearranging, we obtain system dynamics in explicit form

$$\ddot{x} = \frac{1}{(m_t + m_h + m_c)} \begin{pmatrix} (m_h + m_c) l_1 \cos\varphi \ddot{\varphi} + m_c l_2 \cos\theta \ddot{\theta} \\ -b\dot{x} - (m_h + m_c) l_1 \sin\varphi \dot{\varphi}^2 \\ -m_c l_2 \sin\theta \dot{\theta}^2 + u \end{pmatrix} \tag{27}$$

$$\ddot{\varphi} = \frac{1}{l_1\left((m_h + m_c)\cos^2\varphi - (m_t + m_h + m_c)\right)} \cdot \begin{pmatrix} \frac{m_c l_2 \left(m_t \cos(\varphi - \theta) + (m_h + m_c)\sin\varphi \sin\theta\right)}{(m_h + m_c)} \ddot{\theta} \\ +\cos\varphi b\dot{x} + (m_t + m_h + m_c) g \sin\varphi \\ -l_1 (m_h + m_c)\cos\varphi \sin\varphi \dot{\varphi}^2 \\ +\frac{m_c l_2 \left(m_t \sin(\varphi - \theta) + (m_h + m_c)\sin\varphi \cos\theta\right)}{(m_h + m_c)} \dot{\theta}^2 \\ -\cos\varphi u \end{pmatrix} \tag{28}$$

$$\ddot{\theta} = \frac{1}{l_2\left(m_c \cos^2\theta - (m_t + m_h + m_c)\right)} \cdot \begin{pmatrix} l_1 \left(m_t \cos(\varphi - \theta) + (m_h + m_c)\sin\varphi \sin\theta\right)\ddot{\varphi} \\ +l_1 \left((m_h + m_c)\sin\theta \cos\varphi - m_t \sin(\varphi - \theta)\right)\dot{\varphi}^2 \\ +m_c l_2 \cos\theta \sin\theta \dot{\theta}^2 + (m_t + m_h + m_c) g \sin\theta \\ +\cos\theta b\dot{x} - \cos\theta u \end{pmatrix}. \tag{29}$$

If this system dynamics is converted into a first-order mathematical model, six state variables can be obtained, including three components of $\mathbf{q} = [x \quad \varphi \quad \theta]^T$ and their first-time derivatives. Assuming that all system states are measurable, the control problem using multi-level sliding mode technique is investigated in the subsections below.

4.1 Control scheme

Considering the first-level sliding surface composed of three components, each component of s corresponds to a tracking error of a displacement variable and its derivative

$$\mathbf{s} = \begin{bmatrix} s_1 \\ s_2 \\ s_3 \end{bmatrix} = \dot{\mathbf{e}} + \boldsymbol{\lambda}\mathbf{e} = \begin{bmatrix} \dot{x} + \lambda_1 (x - x_d) \\ \dot{\varphi} + \lambda_2 \varphi \\ \dot{\theta} + \lambda_3 \theta \end{bmatrix} \tag{30}$$

where $\boldsymbol{\lambda} = \mathrm{diag}(\lambda_1, \lambda_2, \lambda_3)$ is a strictly positive diagonal matrix. To force state trajectories to reach the first-level sliding surface, Utkin [32] defined the equivalent control input determined from equation $\dot{\mathbf{s}} = \mathbf{0}$. By differentiating expression Eq. (30) with respect to time and making it equally zero, the following equation can be obtained:

$$\dot{s}_1 = \ddot{x} + \lambda_1 \dot{x} = 0;\ \dot{s}_2 = \ddot{\varphi} + \lambda_2 \dot{\varphi} = 0;\ \dot{s}_3 = \ddot{\theta} + \lambda_3 \dot{\theta} = 0\,. \tag{31}$$

By substituting Eqs. (27)-(29) into Eq. (31), we acquire equivalent control inputs as follows

$$\begin{aligned} u_{eq1} = & -(m_h + m_c) l_1 \cos\varphi \ddot{\varphi} - m_c l_2 \cos\theta \ddot{\theta} \\ & + \left(b - \lambda_1 (m_t + m_h + m_c)\right)\dot{x} \\ & + (m_h + m_c) l_1 \sin\varphi \dot{\varphi}^2 + m_c l_2 \sin\theta \dot{\theta}^2 \end{aligned} \tag{32a}$$

$$\begin{aligned} u_{eq2} = & \frac{m_c l_2 \left(m_t \cos(\varphi - \theta) + (m_h + m_c)\sin\varphi \sin\theta\right)}{(m_h + m_c)\cos\varphi} \ddot{\theta} \\ & + b\dot{x} - l_1 (m_h + m_c)\sin\varphi \dot{\varphi}^2 \\ & + (m_t + m_h + m_c) g \tan\varphi \\ & + \frac{m_c l_2 \left(m_t \sin(\varphi - \theta) + (m_h + m_c)\sin\varphi \cos\theta\right)}{(m_h + m_c)\cos\varphi} \dot{\theta}^2 \\ & + \frac{\lambda_2 l_1}{\cos\varphi}\left((m_h + m_c)\cos^2\varphi - (m_t + m_h + m_c)\right)\dot{\varphi} \end{aligned} \tag{32b}$$

$$\begin{aligned} u_{eq3} = & \frac{l_1}{\cos\theta}\left(m_t \cos(\varphi - \theta) + (m_h + m_c)\sin\varphi \sin\theta\right)\ddot{\varphi} \\ & + m_c l_2 \sin\theta \dot{\theta}^2 + b\dot{x} + (m_t + m_h + m_c) g \tan\theta \\ & + \frac{l_1}{\cos\theta}\left((m_h + m_c)\sin\theta \cos\varphi - m_t \sin(\varphi - \theta)\right)\dot{\varphi}^2 \\ & + \frac{\lambda_3 l_2}{\cos\theta}\left(m_c \cos^2\theta - (m_t + m_h + m_c)\right)\dot{\theta} \end{aligned} \tag{32c}$$

Equivalent control input u_{eq1} attracts a pair of state variables $(x, \dot{x})$ to component s_1. Similarly, the duties of u_{eq2} and u_{eq3} are to force the pairs of state variables ($\varphi, \dot{\varphi}$) and ($\theta, \dot{\theta}$) to approach components s_2 and s_3, respectively. Therefore, to drive all state trajectories to reach first-level sliding manifold s, we introduce a total equivalent control input by linearly combining u_{eq1}, u_{eq2}, and u_{eq3} as follows

$$u_{eq} = u_{eq1} + u_{eq2} + u_{eq3} \tag{33}$$

which is expanded to

$$u_{eq} = \begin{pmatrix} \frac{l_1}{\cos\theta}\left(m_t \cos(\varphi - \theta) - (m_h + m_c)\cos(\varphi + \theta)\right)\ddot{\varphi} \\ \frac{m_c l_2}{(m_h + m_c)\cos\varphi}\begin{pmatrix} m_t \cos(\varphi - \theta) \\ -(m_h + m_c)\cos(\varphi + \theta) \end{pmatrix}\ddot{\theta} \\ \frac{\lambda_2 l_1}{\cos\varphi}\left((m_h + m_c)\cos^2\varphi - (m_t + m_h + m_c)\right)\dot{\varphi} \\ (m_t + m_h + m_c) g\left(\tan\varphi + \tan\theta\right) \\ \frac{\lambda_3 l_2}{\cos\theta}\left(m_c \cos^2\theta - (m_t + m_h + m_c)\right)\dot{\theta} \\ \left(3b - \lambda_1 (m_t + m_h + m_c)\right)\dot{x} \\ \frac{l_1}{\cos\theta}\left((m_h + m_c)\sin\theta \cos\varphi - m_t \sin(\varphi - \theta)\right)\dot{\varphi}^2 \\ \frac{m_c l_2}{(m_h + m_c)\cos\varphi}\begin{pmatrix} m_t \sin(\varphi - \theta) \\ +(m_h + m_c)\sin(\varphi + \theta) \\ +(m_h + m_c)\cos\varphi \sin\theta \end{pmatrix}\dot{\theta}^2 \end{pmatrix}. \tag{34}$$

However, discontinuous action u_{sw} must be introduced into Eq. (33) to maintain state motions on the sliding surface, thus overall SMC input becomes

$$u = u_{eq} + u_{sw} = u_{eq1} + u_{eq2} + u_{eq3} + u_{sw}. \tag{35}$$

Discontinuous input u_{sw} normally causes a switching action with sufficiently high frequency to retain all state trajectories moving on manifold $S = 0$ with S, which is referred to as second-level sliding surface. Second-level sliding surface is defined by linearly combining the three components of first-level sliding surface as follows:

$$S = \mu_1 s_1 + \mu_2 s_2 + \mu_3 s_3. \tag{36}$$

More precisely, S denotes the switching line that all system states are attracted to and retained on. The switching action u_{sw} is determined based on the stability of sliding line S. By deriving S with respect to time, one obtains

$$\dot{S} = \mu_1(\ddot{x} + \lambda_1 \dot{x}) + \mu_2(\ddot{\varphi} + \lambda_2 \dot{\varphi}) + \mu_3(\ddot{\theta} + \lambda_3 \dot{\theta}). \tag{37}$$

By substituting Eqs. (27)-(29) and (35) into Eq. (37), and by setting $\dot{S} = -KS - \eta \operatorname{sgn}(S)$, one obtains the switching component

$$u_{sw} = -\frac{1}{f(\mathbf{q})}\left(g(\mathbf{q}, \dot{\mathbf{q}}) + KS + \eta \operatorname{sgn}(S)\right) - u_{eq} \tag{38}$$

where

$$f(\mathbf{q}) = \begin{pmatrix} \dfrac{\mu_1}{(m_t + m_h + m_c)} - \dfrac{\mu_2 \cos\varphi}{l_1\left((m_h + m_c)\cos^2\varphi - (m_t + m_h + m_c)\right)} \\ -\dfrac{\mu_3 \cos\theta}{l_2\left(m_c \cos^2\theta - (m_t + m_h + m_c)\right)} \end{pmatrix}$$

$$g(\mathbf{q}, \dot{\mathbf{q}}) = \begin{pmatrix} \mu_1 \dfrac{\begin{pmatrix} (m_h + m_c) l_1 \cos\varphi \ddot{\varphi} + m_c l_2 \cos\theta \ddot{\theta} \\ -b\dot{x} - (m_h + m_c) l_1 \sin\varphi \dot{\varphi}^2 - m_c l_2 \sin\theta \dot{\theta}^2 \end{pmatrix}}{(m_t + m_h + m_c)} \\ + \mu_2 \dfrac{\begin{pmatrix} m_c l_2 \left(m_t \cos(\varphi - \theta) + (m_h + m_c)\sin\varphi \sin\theta\right)\ddot{\theta} \\ + (m_h + m_c)(m_t + m_h + m_c) g \sin\varphi \\ + m_c l_2 \left(m_t \sin(\varphi - \theta) + (m_h + m_c)\sin\varphi \cos\theta\right)\dot{\theta}^2 \\ - l_1 (m_h + m_c)^2 \cos\varphi \sin\varphi \dot{\varphi}^2 + (m_h + m_c)\cos\varphi b\dot{x} \end{pmatrix}}{l_1 (m_h + m_c)\left((m_h + m_c)\cos^2\varphi - (m_t + m_h + m_c)\right)} \\ + \mu_3 \dfrac{\begin{pmatrix} l_1 \left(m_t \cos(\varphi - \theta) + (m_h + m_c)\sin\varphi \sin\theta\right)\ddot{\varphi} \\ + \cos\theta b\dot{x} + (m_t + m_h + m_c) g \sin\theta \\ + l_1 \begin{pmatrix} (m_h + m_c)\sin\theta \cos\varphi \\ - m_t \sin(\varphi - \theta) \end{pmatrix} \dot{\varphi}^2 + m_c l_2 \cos\theta \sin\theta \dot{\theta}^2 \end{pmatrix}}{l_2\left(m_c \cos^2\theta - (m_t + m_h + m_c)\right)} \\ + \mu_1 \lambda_1 \dot{x} + \mu_2 \lambda_2 \dot{\varphi} + \mu_3 \lambda_3 \dot{\theta} \end{pmatrix}.$$

In the next step, we will prove that both first-level and second-level sliding surfaces are as stable as the following subsection if the system is controlled by HSMC force Eq. (35).

4.2 Stability of sliding surface

We first prove the stability of second-level sliding surface by considering a positive definite Lyapunov function $V = 0.5S^2$. The first-order derivative of V is in the form

$$\dot{V} = S\dot{S} = S\left(-KS - \eta \operatorname{sgn}(S)\right) = -KS^2 - \eta|S|. \tag{39}$$

Because $\dot{V} \le 0$ for every $K > 0$ and $\eta > 0$, second-level surface S is bounded. Therefore, Lyapunov function V is lower bounded. Second-order derivative of V is

$$\begin{aligned} \ddot{V} &= \dot{S}^2 + \ddot{S}S = \left(KS + \eta \operatorname{sgn}(S)\right)^2 - K\dot{S}S \\ &= K^2S^2 + \eta^2 + 2\eta K|S| + K^2S^2 + \eta K|S| \\ &= 2K^2S^2 + \eta^2 + 3\eta K|S| \end{aligned} \tag{40}$$

which is bounded for every finite positive numbers K and η. This step yields function V which is uniformly continuous in time. Lyapunov function V satisfies all the conditions of Barbalat's lemma; therefore, if $\lim_{t\to\infty} \dot{V} = 0$, then $\lim_{t\to\infty}\left(-KS^2 - \eta|S|\right) = 0$, which means $\lim_{t\to\infty} S = 0$. Thus, we can conclude that second-level surface S is asymptotically stable.

The stability of the first-level sliding surface is then investigated. Based on physical insight, the pair of system states (φ, θ) always reach equilibrium point (0,0) because of gravity. This event leads to

$$\lim_{t\to\infty} s_2 = \lim_{t\to\infty} s_3 = \lim_{t\to\infty}\left(\ddot{\varphi} + \lambda_2 \dot{\varphi}\right) = \lim_{t\to\infty}\left(\ddot{\theta} + \lambda_3 \dot{\theta}\right) = 0. \tag{41}$$

Expressions Eqs. (36) and (41) yields

$$\lim_{t\to\infty} s_1 = \frac{-\lim_{t\to\infty} \mu_2 s_2 - \lim_{t\to\infty} \mu_3 s_3}{\mu_1} = 0. \tag{42}$$

Therefore, first-level sliding surface s is asymptotically stable. Wang completely proved the stability of first-level sliding surface of a class of SIMO systems from a mathematical point of view in Ref. [25].

5. Numerical simulation and its results

System dynamics Eq. (4) driven by either CSMC-based Eq. (8) or HSMC-based controller Eq. (35) is numerically simulated. Physical parameters of the system and the parameters of the controllers are described in Table 1.

Simulation results are illustrated in Figs. 2-10. Sliding manifolds of system-corresponding CSMC and HSMC techniques are depicted in Figs. 2-3. Reach time of CSMC-based sliding manifold is approximately 2 sec (Fig. 2), whereas

Table 1. Design parameters.

System dynamics	CSMC-based controller	HSMC-based controller
$m_t = 50$ kg; $m_c = 2$ kg; $m_h = 10$ kg; $l_1 = 3$ m; $l_2 = 0.3$ m; $b = 90$ N.s/m; $g = 9.81$ m/s^2; $\left(x_0, \dot{x}_0, \varphi_0, \dot{\varphi}_0, \theta_0, \dot{\theta}_0\right)$; $= (0,0,0,0,0,0)$	$x_d = 4$ m; $K = 70$; $\lambda = 0.5$; $\alpha = 17$; $\beta = -11$;	$x_d = 4$ m; $K = 1.5$; $\eta = 10$; $\lambda_1 = 0.35$; $\lambda_2 = 22$; $\lambda_3 = 50$; $\mu_1 = 1.18$; $\mu_2 = 1.2$; $\mu_3 = -0.35$;

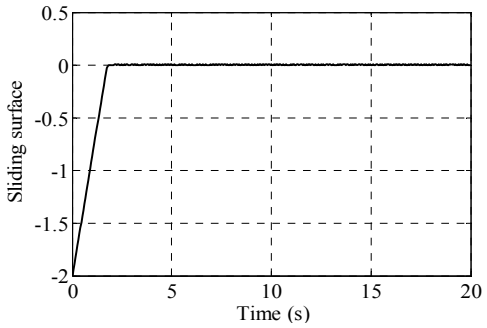

Fig. 2. Sliding surface of CSMC.

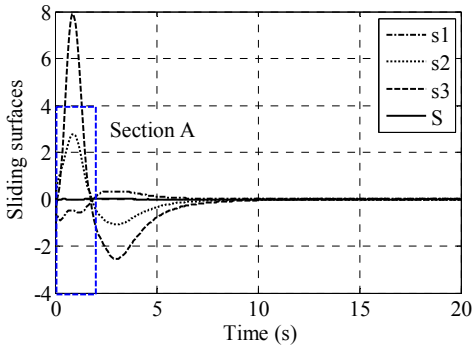

(a)

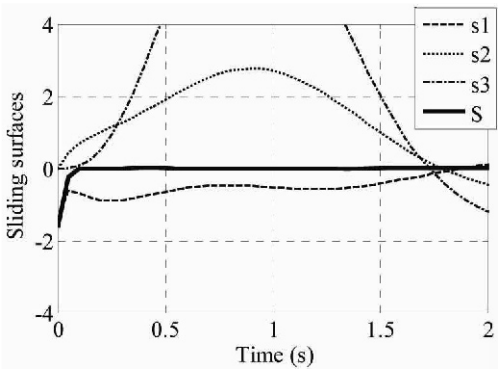

(b)

Fig. 3. (a) Sliding surfaces of HSMC; (b) The enlarged view of Fig. 3(a).

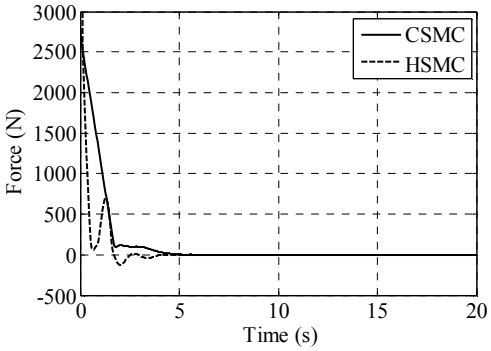

Fig. 4. Trolley driving force.

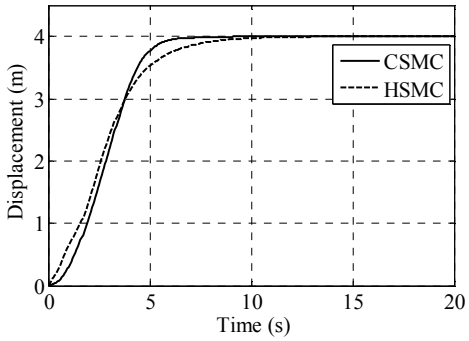

Fig. 5. Trolley displacement.

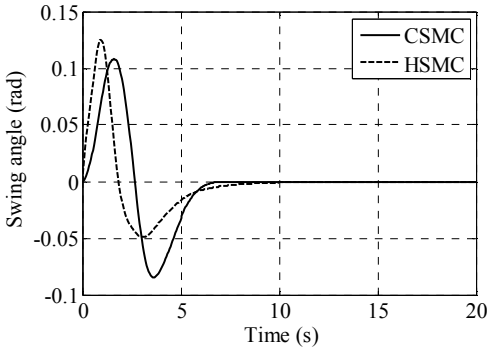

Fig. 6. Swing angle of hook.

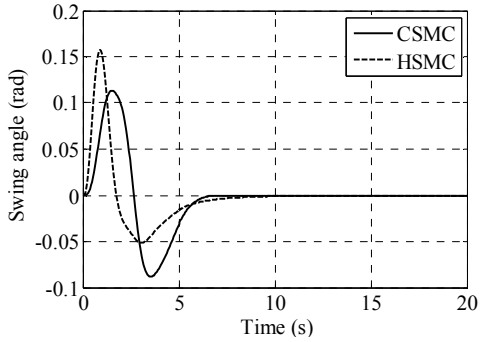

Fig. 7. Swing angle of cargo.

that of HSMC-based primary manifold is small, at roughly 0.1 sec (Fig. 3). Theoretically, the shorter the period of reaching phase of the sliding manifold is, the more robust the crane system becomes [33]. Therefore, as we will see later, robustness of HSMC-based responses are better than those of CSMC-based responses.

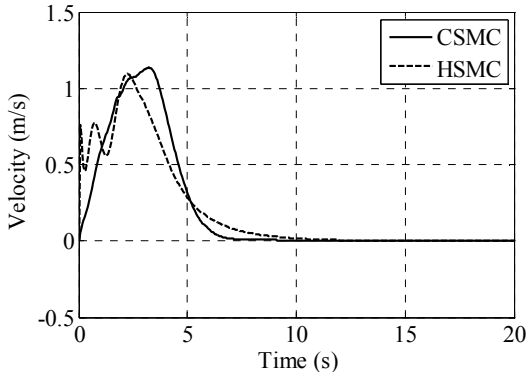

Fig. 8. Trolley velocity.

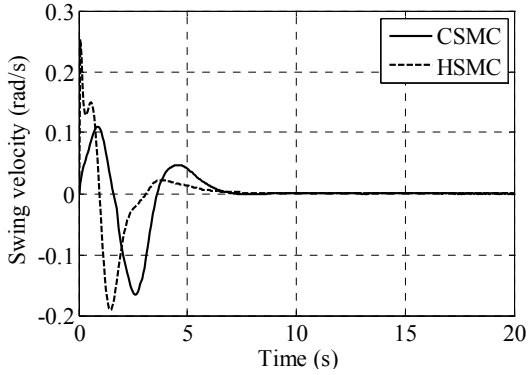

Fig. 9. Swing velocity of hook.

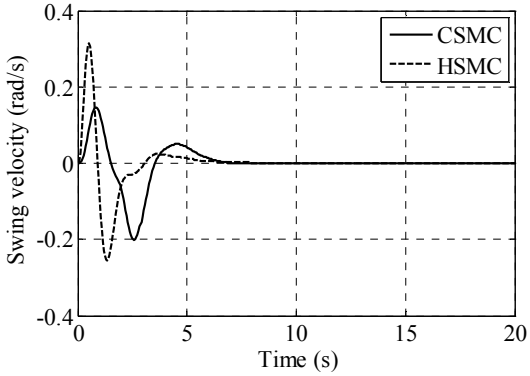

Fig. 10. Swing velocity of cargo.

It is shown in Fig. 5 that the path of the trolley motion in which CSMC response is smoother than that of HSMC response. Both responses regularly approach the desired value without overshooting. CSMC response reaches a steady-state after 9.7 sec, whereas setting time of HSMC response is about 14.3 sec. Hook and cargo swings are described in Figs. 6 and 7, respectively, in which qualities of CSMC-based responses are better than those of HSMC-based responses. Cargo swing vanishes completely after 6.8 sec for CSMC, and 12.2 sec for HSMC.

SMC and its modified versions are known to be robust. Their robustness results from their intrinsic capability to deal

Table 2. Comparison of response specifications.

Techniques		Nominal values of uncertainties			Increasing 50 % values of uncertainties	
		CSMC	HSMC	PBC [37]	CSMC	HSMC
Hook swing angle	Setting time (sec)	7.03	14.41	33	6.77	12.82
	Maximum swing angle, φ_{max} (degree)	6.19	7.18	13	4.42	10.93
Cargo swing angle	Setting time (sec)	6.81	12.2	34	6.76	13.12
	Maximum swing angle, θ_{max} (degree)	6.51	9.04	16	4.68	8.08
Trolley displacement	Setting time (sec)	9.705	14.3	31	6.85	14.63
	Maximum overshoot (%)	0	0	0	0	0

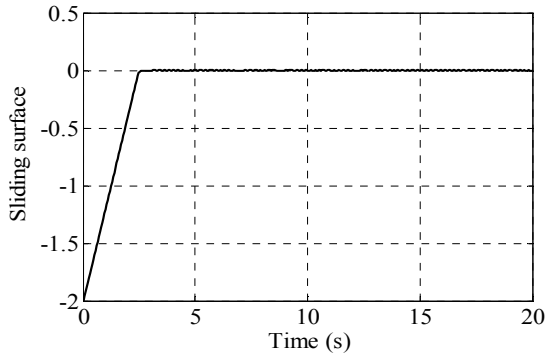

Fig. 11. Sliding surface of CSMC with uncertainties.

with uncertain components [34]. To investigate robustness of a crane system with respect to variations of its inherent physical parameters, which are viewed as uncertainties, we retain all design parameters of both CSMC and HSMC controllers but increases values of uncertainties: $\Delta l_1 = \Delta l_2 = \Delta m_c = \Delta m_t = 50$ %. System responses simulated in the presence of parameter perturbations are shown in Figs. 11-19. Robustness of both CSMC-based and HSMC-based responses is presented in Table 2, in which response specifications in cases of presence and absence of parameter disturbance are described. Both CSMC-based and HSMC-based state trajectories are robust. However, HSMC-based responses are more robust than CSMC-based responses because time to reach second-level surface using HSMC technique is shorter than that of CSMC-based technique. Table 2 shows that CSMC response specifications vary more than HSMC response specifications when values of uncertainties increased. Comparing Figs. 5-7 with Figs. 14-16, respectively, we easily see that HSMC-based responses exhibited less change in shapes than CSMC-based responses. Qualities of HSMC-based responses appear to be better than those of CSMC-base responses. In summary, both CSMC and HSMC controllers guarantee asymptotical stability of all system responses even when the physical structure of the system is

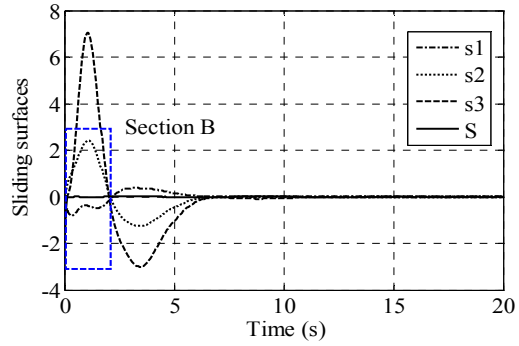

(a)

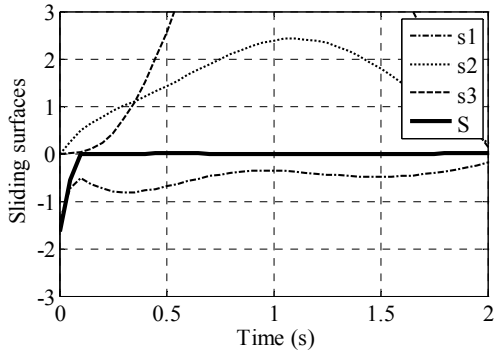

(b)

Fig. 12. (a) Sliding surfaces of HSMC with uncertainties; (b) Zoom out of section B of Fig. 12(a).

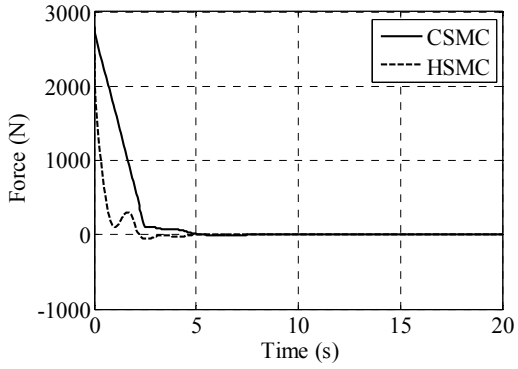

Fig. 13. Trolley driving force with uncertainties.

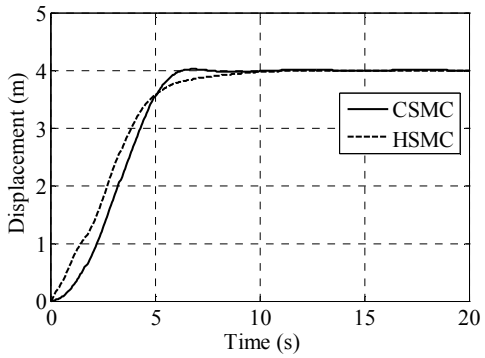

Fig. 14. Trolley displacement with uncertainties.

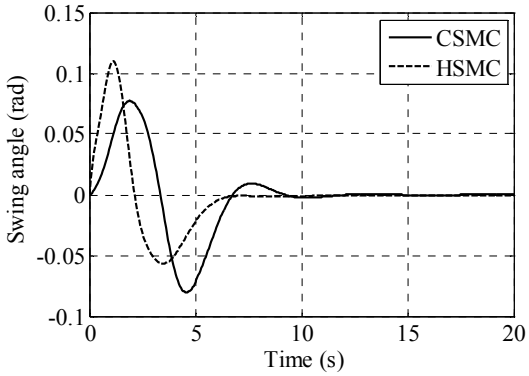

Fig. 15. Swing angle of hook with uncertainties.

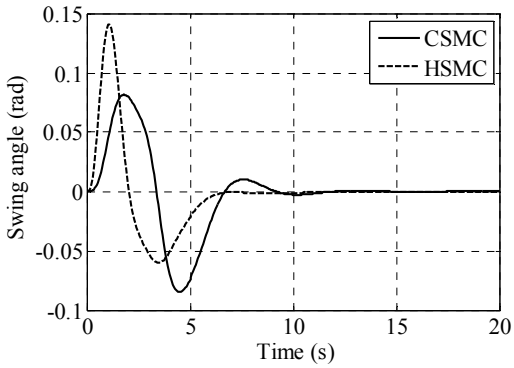

Fig. 16. Swing angle of cargo with uncertainties.

varied; however, HSMC controller is more robust than CSMC controller. Comparison among CSMC, HSMC, and passivity-based control (PBC) [37] is shown in Table 2. All specifications of CSMC and HSMC appear to be better than those of PBC. Both settling time and maximum swing angles of CSMC and HSMC are considerably smaller than those of PBC.

6. Conclusions

Two robust controllers were designed for both tracking and anti-swing control of double-pendulum overhead cranes using SMC technique and a modified version. Both controllers worked well and stabilized overall crane system. Movement of the trolley and its stoppage were controlled precisely at its destination. Concurrently, both hook and cargo swings were kept small during the transfer process and were completely suppressed after a considerably short time. Simulation results also demonstrated that responses of the crane system driven by the proposed controllers were robust even when several physical parameters of the system were changed. In a particular simulation case, HSMC-based controller was more robust than CSMC controller because the reaching period of HSMC-based controller was shorter than that of CSMC-based controller. To improve robustness of the system, optimum design of the sliding manifold will be carried out in our future work to minimize or cancel out the reaching period.

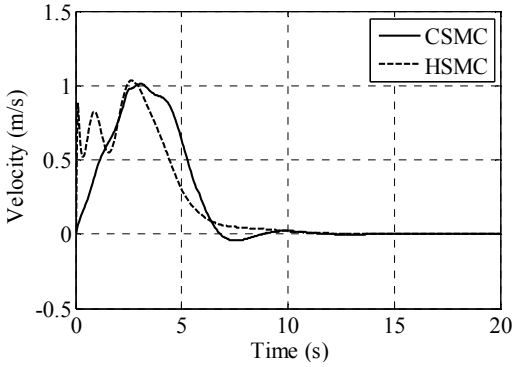

Fig. 17. Trolley velocity with uncertainties.

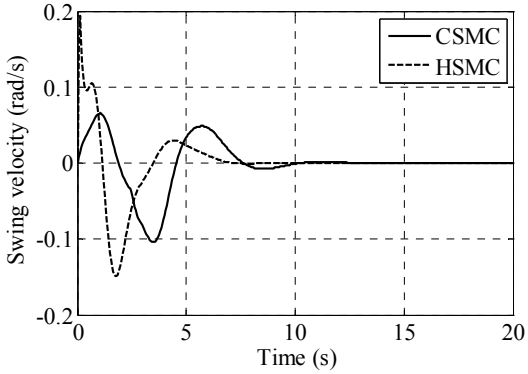

Fig. 18. Swing velocity of hook with uncertainties.

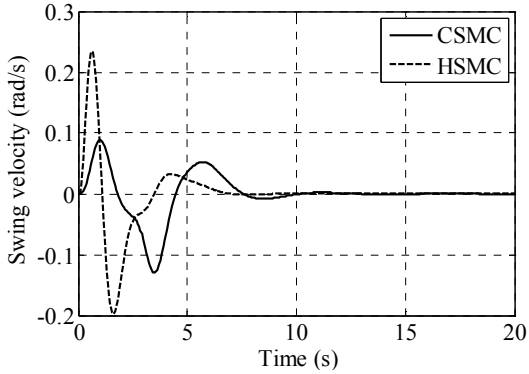

Fig. 19. Swing velocity of cargo with uncertainties.

Acknowledgment

This research was partially supported by the Ministry of Knowledge Economy (MKE) of South Korea with supervision from the Korea Evaluation Institute of Industrial Technology (KEIT) (Grant No. 10041629, Implementation of Technologies for Identification, Behavior, and Location of Human based on Sensor Network Fusion Program), as well as MKE under the IT R&D program of KEIT (Grant No. KI10040990, A Development of Communication Technology with UTIS & Vehicle Safety Support Service for Urban Area). It was also supported by the Technology Innovation Program (10040992) of MKE/KEIT.

References

[1] Y. Sakawa and H. Sano, Nonlinear model and linear robust control of overhead travelling cranes, *Nonlinear Analysis, Theory, Methods & Applications*, 30 (4) (1997) 2197-2207.

[2] O. Sawodny, H. Aschemann and S. Lahres, An automated gantry crane as a large workspace robot, *Control Engineering Practice*, 10 (12) (2002) 1323-1338.

[3] A. Giua, C. Seatzu and G. Usai, Observer-controller design for cranes via Lyapunov equivalence, *Automatica*, 35 (4) (1999) 669-678.

[4] T. A. Le, G. H. Kim, M. Y. Kim and S. G. Lee, Partial feedback linearization control of overhead cranes with varying cable lengths, *International Journal of Precision Engineering And Manufacturing*, 13 (4) (2012) 501-507.

[5] L. A. Tuan, V. H. Dang, D. H Ko, T. N. An and S. G. Lee, Nonlinear controls of a rotating tower crane in conjunction with trolley motion, *Journal of Systems and Control Engineering*, first published on April 16, 2013 as DOI: 10.1177/0959651812472437.

[6] L. A. Tuan, S. C. Moon, W. G. Lee and S. G. Lee, Adaptive sliding mode control of overhead cranes with varying cable length, *Journal of Mechanical Science and Technology*, 27 (3) (2013) 885-893.

[7] H. Park, D. Chwa and K. S. Hong, A feedback linearization control of Container cranes: Varying rope length, *International Journal of Control, Automation, and Systems*, 5 (4) (2007) 379-387.

[8] L. A. Tuan, S. G. Lee, V. H. Dang, S. C. Moon and B. S. Kim, Partial feedback linearization control of a three-dimensional overhead crane, *International Journal of Control, Automation, and Systems* (2013) (Accepted).

[9] C. C. Cheng and C. Y. Chen, Controller design for an overhead crane system with uncertainty, *Control Engineering Practice*, 4 (5) (1996) 645-653.

[10] H. C. Cho, J. W. Lee, Y. J. Lee and K. S. Lee, Lyapunov theory based robust control of complicated nonlinear mechanical systems with uncertainty, *Journal of Mechanical Science and Technology*, 22 (11) (2008) 2142-2150.

[11] C. S. Kim and K.S. Hong, Boundary control of container cranes from perspective of controlling an axially moving string system, *International Journal of Control, Automation, and Systems*, 7 (3) (2009) 437-445.

[12] Y. S. Kim, K. S. Hong and S. K. Sul, Anti-sway control of container cranes: inclinometer, observer, and state feedback, *International Journal of Control, Automation, and Systems*, 2 (4) (2004) 435-449.

[13] Y. Fang, W. E. Dixon, D. M. Dawson and E. Zergeroglu, Nonlinear coupling control laws for an under-actuated overhead crane system, *IEEE/ASME Transactions on Mechatronics*, 8 (3) (2003) 418-423.

[14] D. Chwa, Nonlinear tracking control of 3D overhead cranes against the initial swing angle and variation of payload weight, *IEEE Transactions on Control Systems Technology*, 17 (4) (2009) 876-883.

[15] K. A. F. Moustafa, Reference trajectory tracking of overhead cranes, *Journal of Dynamic Systems, Measurement, and Control*, 123 (1) (2001) 139-141.
[16] K. Lee, S. Coates and V. C. Carroll, Variable structure control applied to under-actuated robots, *Robotica*, 15 (3) (1996) 313-318.
[17] H. Ashrafiuon and R. S. Erwin, Sliding mode control of under-actuated multi-body systems and its application to shape change control, *International Journal of Control*, 81 (12) (2008) 1849-1858.
[18] V. Sankaranarayanan and A. D. Mahindakar, Control of a class of under-actuated mechanical systems using sliding modes, *IEEE Transactions on Robotics*, 25 (2) (2009) 459-466.
[19] M. A. Karkoub and M. Zribi, Robust control schemes for an overhead crane, *Journal of Vibration and Control*, 7 (3) (2001) 395-416.
[20] G. Bartolini, A. Pisano and E. Usai, Output-feedback control of container cranes: A comparative analysis, *Asian Journal of Control*, 5 (4) (2003) 578-593.
[21] Q. H. Ngo and K. S. Hong, Sliding mode anti-sway control of an offshore container crane, *IEEE/ASME Transactions on Mechatronics*, 17 (2) (2012) 201-209.
[22] G. Bartolini, A. Pisano and E. Usai, Second-order sliding mode control of container cranes, *Automatica*, 38 (10) (2002) 1783-1790.
[23] H. H. Lee, Y. Liang and D. Segura, A sliding mode anti-swing trajectory control for overhead cranes with high-speed load hoisting, *Journal of Dynamics Systems, Measurement, and Control*, 128 (4) (2006) 842-845.
[24] N. Almutairi and M. Zribi, Sliding mode control of a three dimensional overhead crane, *Journal of Vibration and Control*, 15 (11) (2009) 1679-1730.
[25] W. Wang, J. Yi, D. Zhao and D. Liu, Design of a stable sliding mode controller for a class of second order underactuated systems, *Proc. of IEEE Conference on Control Theory Application*, Beijing, China (2004) 683-690.
[26] D. Qian, J. Yi and D. Zhao, Multi layers sliding mode control for a class of under-actuated systems, *Proc. of IMACS Multi-conference on Computational Engineering in Systems Applications*, Beijing, China (2006) 530-535.
[27] D. Qian, J. Yi, D. Zhao and Y. Hao, Hierarchical sliding mode control for series double inverted pendulums system, *Proc. of the 2006 IEEE/RSJ, International Conference on Intelligent Robots and Systems*, Beijing, China (2006) 4977-4982.
[28] D. Qian, J. Yi and D. Zhao, Hierarchical sliding mode control to swing up a pendubot, *Proc. of the 2007 American Control Conference*, New York, USA (2007) 5254-5259.
[29] A. Khalid, J. Huey, W. Singhose, J. Lawrence and D. Frakes, Human operator performance testing using an input-shaped bridge crane, *ASME J. of Dynamic Systems, Measurement, and Control*, 128 (4) (2006) 835-841.
[30] R. Xu, *Optimal sliding mode control and stabilization of under-actuated systems*, PhD Thesis, Ohio State University, Ohio, USA (2007).
[31] J. J. E. Slotine and W. Li, *Applied nonlinear control*, Prentice Hall, Englewood Cliffs, NJ, USA (1991).
[32] V. Utkin, J. Guldner and J. Shi, *Sliding mode control in electromechanical systems*, Second Ed. Taylor & Francis, USA (2009).
[33] S. G. Sajad and B. H. Mohammad, Optimal design of rotating sliding surface for sliding mode control, *Proc. of the American Control Conference*, St. Louis, MO, USA (2009) 774-777.
[34] G. Bartolini, N. Orani, A. Pisano and E. Usai, Load swing in overhead cranes by sliding mode technique, *Proc. of the 39th IEEE Conference on Decision and Control*, Sydney, Australia (2000) 1697-1702.
[35] M. A. Ahmad, R. Ismail, M. S. Ramli, A. N. Nasir and N. Hambali, Feed-forward techniques for sway suppression in a double-pendulum-type overhead crane, *Proc. of International Conference on Computer Technology and Development*, Kota Kinabalu, Malaysia (2009) 173-178.
[36] G. Yang, W. Zhang, Y. Huang and Y. Yu, Simulation research of extension control based on crane-double pendulum system, *Journal of Computer and Information Science*, 2 (1) (2009) 103-107.
[37] G. Weiping, L. Diantong, Y. Jianqiang and Z. Dongbin, Passivity-based-control for double-pendulum-type overhead cranes, *Proc. of the IEEE Region 10 Conference*, Chiang Mai, Thailand (2004) 546-549.

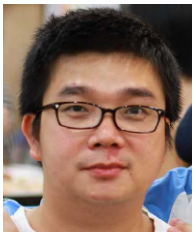

Le Anh Tuan graduated both B.E. and M.E. in Mechanical Engineering and Marine Machinery from Vietnam Maritime University in 2003 and 2007, respectively. He received the Ph.D. degree in Mechanical Engineering from Kyung Hee University, South Korea in 2012. He is a part-time researcher of Duy Tan University, Da Nang, Vietnam. His interested research composes of applied nonlinear control, dynamics and control of industrial machines.

Soon-Geul Lee received his B.E. degree in Mechanical Engineering from Seoul National University, Seoul, Korea; his M.S. degree in Production Engineering from KAIST, Seoul, Korea; and his Ph.D. degree in Mechanical Engineering from the University of Michigan in 1983, 1985 and 1993 respectively. Since 1996, he has been with the Department of Mechanical Engineering of Kyung Hee University, Yongin, Korea, where he is currently a Professor. His research interests include robotics and automation, mechatronics, intelligent control, and biomechanics. He likewise served as the Director of the Korean Society of Precision Engineering (KSPE) (2005-2007) and for the Institute of Control, Automation, and Systems Engineers (ICASE) (2006).